Journal of Applied Physics | ARTICLE | pubs.aip.org/aip/jap

At wavelength metrology of high-reflectance multilayer mirror in the water window

Cite as: J. Appl. Phys. **139**, 013107 (2026); doi: 10.1063/5.0310891
Submitted: 5 November 2025 · Accepted: 13 December 2025 ·
Published Online: 6 January 2026

Franck Delmotte,[1,2,a)] Evgueni Meltchakov,[1] Andrey Sokolov,[3] Pascal Mercère,[4] Blandine Capitanio,[4] and Eric Gullikson[2]

AFFILIATIONS

[1]Institut d'Optique Graduate School, CNRS, Laboratoire Charles Fabry, Université Paris-Saclay, Palaiseau, France
[2]Center for X-ray Optics, LBNL, Berkeley, California 94720, USA
[3]Helmholtz-Zentrum Berlin, BESSY II, Berlin, Germany
[4]Synchrotron Soleil, L'Orme des Merisiers, Université Paris-Saclay, Départementale 128, Saint-Aubin 91190, France

[a)]**Author to whom correspondence should be addressed:** franck.delmotte@institutoptique.fr

ABSTRACT

Multilayer mirrors for the water window spectral range (photon energies from 284 to 543 eV, which correspond, respectively, to the C–K and O–K absorption edges) have become key components for microscopy, synchrotron and free electron laser sources, semiconductor microanalysis, and x-ray spectroscopy. The emergence of new x-ray sources and new applications in this spectral domain (e.g., soft x-ray photolithography and attosecond science) requires more efficient optical components with precise metrology of their performance. We have recently reported high experimental peak reflectance at near-normal incidence near the Sc $L_{2,3}$ absorption edge (E ≈ 400 eV) by the experimental optimization of Cr/Sc-based multilayers. The short wavelength and the large number of multilayer periods raise some specific issues for the at-wavelength reflectance measurements. We report here on a systematic study of potential bias in the measurements of high-reflectance multilayer mirror in the water window based on a comparison between experimental data from the three different synchrotron beamlines as well as theoretical calculations and simulations. In particular, we discuss the effects of spectral resolution and angular resolution on the peak reflectance as well as the influence of the sample lateral uniformity and of the light scattered by the multilayer sample (diffuse scattering). As a result of this study, we determined the peak reflectance of this multilayer mirror to be 35% at E = 396 eV at near-normal incidence, which is the highest reflectance reported in the water window spectral range.

I. INTRODUCTION

Multilayer mirrors have become key components for a large variety of applications from the extreme ultraviolet (EUV) to the hard x-ray spectral domains. Due to Bragg's law, the period of the multilayer needs to be about half of the operating wavelength for normal incidence optics. Hence, the development of multilayers with ultra-short period has pushed the limit of efficient near-normal incidence optics toward short wavelengths, especially in the water window (WW), a spectral region delimited by the K absorption edges of C and O atoms (284–543 eV), which is of great interest for microscopy, biological imaging, semiconductor industry, synchrotron and free electron laser sources, and attosecond science.[1–9]

In 1997, Salashchenko and Shamov reported the first experimental results with Cr/Sc multilayers with near-normal incidence reflectance greater than 10% for photon energy below the Sc $L_{2,3}$ absorption edges (∼400 eV).[1] Although this value represented a huge improvement compared to the previous WW multilayer mirrors, it remains very far from the theoretical value calculated for an ideal Cr/Sc multilayer stack (∼60%). This is because of the dramatic effect of interfacial roughness in these multilayers with ultra-short periods.[10]

Numerous studies aiming at reducing interfacial defects in the Sc-based multilayer for the WW (and thus improving the reflectance) have been conducted by several groups, yet most of the reported experimental reflectance remained below 20%.[11–13] One notable exception is the value of 32% obtained by Gullikson *et al.*

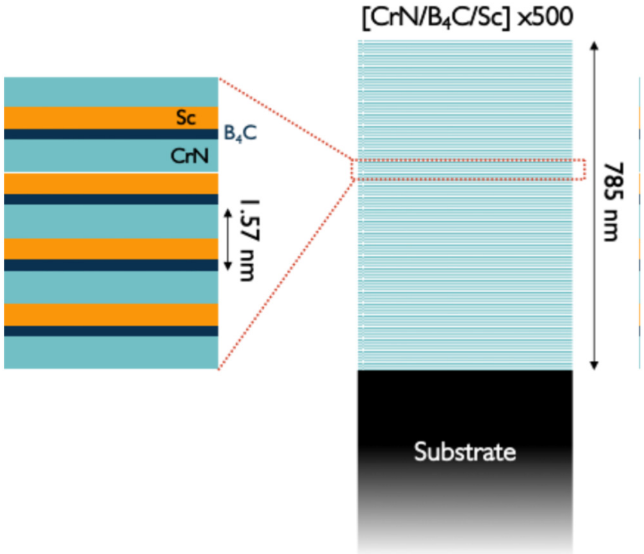

FIG. 1. Schematic of the $CrN/B_4C/Sc$ multilayer coating. The coating ends with a B_4C capping layer (not shown).

by introducing B_4C barrier layers in a Cr/Sc multilayer and presented at the Physics of X-ray Multilayer Structure Conference in 2006.[14] Other interface engineering methods described in the previous studies included the nitridation of the Cr and/or Sc layers.[15] In 2017, we proposed a new multilayer structure by combining the addition of a thin B_4C barrier layer at the Sc-on-Cr interface and the nitridation of the Cr layer, and we measured a peak reflectance of 23%.[16] By further optimization of the layer thicknesses and of the deposition parameters, we reported in 2024 a peak reflectance of 32% for a $CrN/B_4C/Sc$ multilayer with 500 periods of ∼1.57 nm.[17] A schematic of this sample, named MP23034, is represented in Fig. 1. An additional B_4C capping layer is added on top of the multilayer (not shown in Fig. 1). As described in Ref. 17, sample MP23034 has been deposited by magnetron sputtering in a Plassys MP800 equipment and its reflectance was measured at 2.5° incidence at SOLEIL XUV Metrology beamline. The surface roughness of the Si substrate before deposition is ∼0.2 nm rms. Reflectance measurements of the same sample at advanced light source (ALS) 6.3.2 beamline and at BESSY II Optics beamline provide peak values R_{peak} of ∼35% and 34%, respectively (Fig. 2). The ALS and BESSY spectra shown in Fig. 2 were measured about 1 year after the initial SOLEIL spectra. In order to check that the sample did n't evolve over this period of time, we remeasure sample MP23034 at SOLEIL after the ALS measurements and we found the same value of R_{peak} when using the same parameters. This confirms the good temporal stability of $CrN/B_4C/Sc$ coatings that we have previously demonstrated over a period of 7 years.[17]

In this paper, we present a systematic study of potential bias in the measurements of high-reflectance multilayer mirror in the WW based on a comparison between experimental data from the three different beamlines as well as theoretical calculations and simulations. After a brief description of the experimental setup for the three beamlines, we present the effect of spectral resolution and then angular resolution on the peak reflectance. The influence of the lateral uniformity of the sample and of the light scattered by the multilayer sample (diffuse scattering) is also discussed.

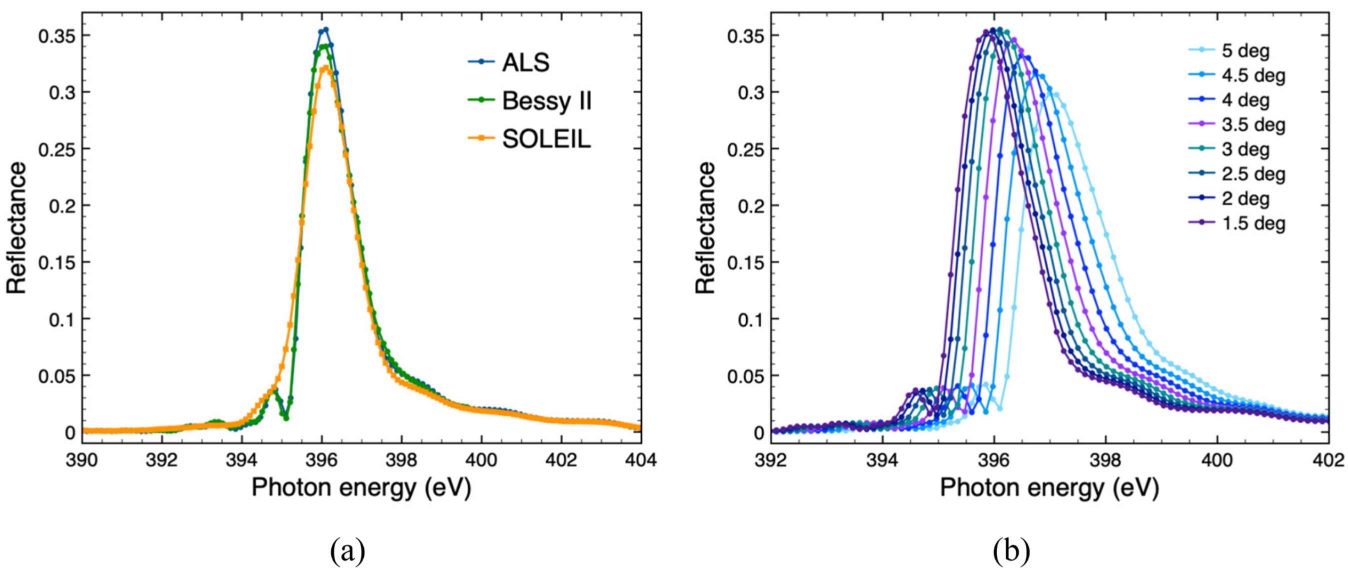

FIG. 2. Reflectance spectra of sample MP23034 measured (a) at three different synchrotron beamlines at 2.5° incidence, and (b) at ALS beamline 6.3.2 for different incident angles.

TABLE I. Main characteristics of the three synchrotron beamlines used in this study for measurements in the spectral range 380–410 eV. The parameters used for the measurements in Fig. 2 are in bold. The spot size on the sample corresponds to the full width at half maximum.

	SOLEIL XUV metro.	ALS 6.3.2	BESSY II optics BL
Grating	300 l/mm	1200 l/mm	1200 l/mm
Exit slit	100–**200** μm	20–**50** μm	50–**100** μm
Filter	0.4 μm Ti	0.6 μm Ti	No filter
Order sorter	Cr at 3°(×2) and 6°	Ni at 3.25° (×2) and 6.5°	Si at 2.6°(×4)
Spot on sample (V × H)	$150 \times 250\,\mu m^2$	$120 \times 40\,\mu m^2$	$350 \times 250\,\mu m^2$
Beam divergence (V × H)	0.7×0.3 mrad^2	1×1 mrad^2	0.5×1.4 mrad^2
Sample–detector distance	290 mm	236 mm	305 mm
Photodiode aperture	10×10 mm^2	**10 × 10 mm^2**, and 4 mm diam.	4 mm diam.

II. DESCRIPTION OF THE BEAMLINES

The three beamlines are operating on a bending magnet. Their optical layouts have been described previously in Refs. 18–22. The main characteristics of interest for the present study are summarized in Table I.

For the measurements at SOLEIL XUV Metrology beamline, we used a 300 lines/mm grating with an exit slit of 200 μm. The high orders of the grating are suppressed by a 0.4 μm thick Ti filter and two reflections at 3° and one at 6° on Cr (order sorter). For the measurements at ALS 6.3.2 beamline, we used a 1200 lines/mm grating with 20 or 50 μm exit slit. The order sorter consists of two reflections at 3.25° and one at 6.5° on Ni, and we used a 0.6 μm thick Ti filter. For the measurements at BESSY II Optics beamline, we used a 1200 lines/mm grating with a 100 μm exit slit. This beamline uses a high-order suppression system based on four reflections from Si mirrors. It has been demonstrated that high spectral purity can be reached with this system without inserting a metallic filter.[21]

As described in Table I, the spot size on the sample varies from 120×40 to $350 \times 250\,\mu m^2$ depending on the beamline. The beam vertical divergence is below 1 mrad for the three beamlines. The initial photodiode apertures (which correspond to the measurements plotted in Fig. 2) were 10×10 mm^2 for SOLEIL and ALS and 4 mm in diameter for BESSY II.

For the 3 beamlines, the monochromator calibration is verified by measuring the $L_{2,3}$ edge of a Ti filter (at $E \approx 453$ eV) prior to each run of reflectance measurements.

Additionally, an absolute energy calibration was performed at BESSY II and at ALS by measuring the N_2 K-edge absorption spectrum at $E \approx 400$ eV. The accuracy of the energy calibration is about 0.02 eV.[21]

The experimental repeatability has been estimated by six successive measurements of the multilayer sample reflectance at ALS 6.3.2 beamline. We obtained a repeatability Dl of ±0.062 pm (standard deviation) in wavelength positioning at l = 3.11 nm and a repeatability DR/R of ±0.08% in peak reflectance. Note that the photodiode non-uniformity is responsible for a significant portion of the 0.08% repeatability: we measured a standard deviation of the photodiode signal as a function of beam position on the diode of about ±0.05%, in this wavelength range. These repeatability and non-uniformity values are similar to the ones determined previously at 13.5 nm wavelength at ALS beamline 6.3.2.[20]

A small portion of the incident beam may not be at the desired wavelength. Those photons could originate from either higher orders or diffused scattering from the monochromator grating.[20] This spectral contamination usually induces a reduction in the measured R_{peak} because those photons are present in the direct beam but are not reflected efficiently by the multilayer mirror.

The high-order suppression system used at BESSY II has been demonstrated to suppress the grating high orders with a remaining contamination in the range of 10^{-7} in the water window spectral range.[21] The spectral contamination due to high-orders and diffuse scattering at ALS has been previously evaluated to be about 1% in the Cr–L edge region ($E \approx 574$–590 eV).[23] In addition, the spectral purity of ALS and SOLEIL beamlines was estimated qualitatively in the Ti–L edge region by comparing the intensity measured through the Ti filter of each beamline. The thickness of each filter being different (400 nm at SOLEIL and 600 nm at ALS), we normalized the signal to 1 for a photon energy of 450 eV. At photon energies above the Ti $L_{2,3}$ edge, the filter becomes strongly absorbing (see simulation in Fig. 3) and the measured signal is mainly due to

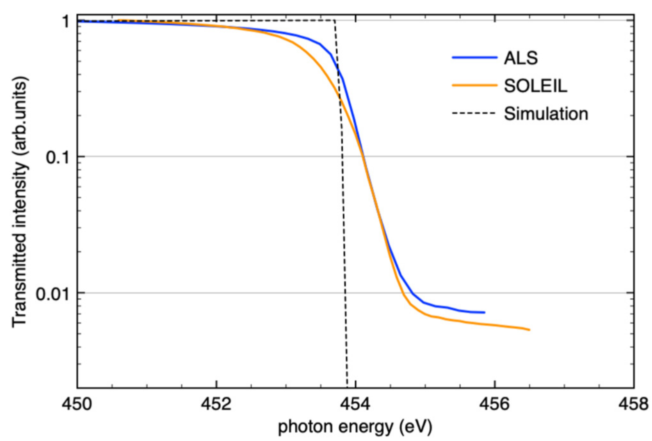

FIG. 3. Transmitted intensity measured through the Ti filter of ALS and SOLEIL beamlines. In both cases, the signal is normalized to 1 at E = 450 eV. The simulated transmission through a 600 nm Ti filter is also plotted for comparison (dashed line).

spectral contamination with higher photon energy, which can still pass through the filter. Thus, the value of the intensity above the edge can provide a rough qualitative estimation of the spectral contamination.[20] As shown in Fig. 3, both SOLEIL and ALS transmitted signals go down below 0.01 at photon energies above 455 eV. This suggests that the spectral contamination is of the same order of magnitude for both beamlines. In consequence, the spectral contamination cannot be responsible for the lower reflectance measured at SOLEIL.

These results imply that the spectral purity is high enough to measure the reflectance with a precision better than 1% relative, which is much lower than the differences observed in Fig. 2.

III. EFFECT OF SPECTRAL RESOLUTION

We consider here the spectral resolution as E/DE with DE the full width at half maximum (FWHM) of the instrumental response. Using IMD software[24] and optical constants from the CXRO database,[25] we calculated the effect of the spectral resolution on the value of peak reflectance for the $CrN/B_4C/Sc$ sample described in Fig. 1. In Fig. 4, we plot the normalized reflectance (1 = infinite spectral resolution) as a function of spectral resolution. This calculation shows that experimental measurement with less than 1% error in the determination of R_{peak} requires a spectral resolution higher than 1550.

The theoretical spectral resolution at ALS 6.3.2 beamline reaches 6000, 3400, and 2200 for an exit slit of 10, 20, and 50 μm, respectively. We confirmed experimentally the spectral resolution with a N_2 gas cell by measuring the vibrational state of the N_2 K-edge absorption spectrum. The pressure in the gas cell during the experiment was set to ∼6 Pa. The experimental data were fitted using a sum of seven Voigt functions (Fig. 5). The Voigt function corresponds to a convolution of a Lorentzian function and a Gaussian function. In this model, the Lorentzian distribution accounts for the natural lifetime width of the vibrational state and the Gaussian distribution accounts for the instrumental resolution. The best fit was obtained with a FWHM of 130 and 77.8 meV, respectively, for the Lorentzian and the Gaussian functions. The value of 130 meV fitted for the natural lifetime width is within the range of values reported in the literature (see, e.g., Table 8 in Ref. 26). Note, however, that these Lorentzian FWHM values have been found dependent on experimental conditions.[27] From these measurements, we can deduce that the spectral resolution E/DE of ALS 6.3.2 beamline at 400 eV photon energy and with an exit slit of 10 μm is about 5150. This value is close to the theoretical resolution calculated for a 10 μm slit. Thus, we can conclude that the spectral resolution for the measurements at ALS (with the exit slit at 20 or 50 μm) was higher than the limit of 1550.

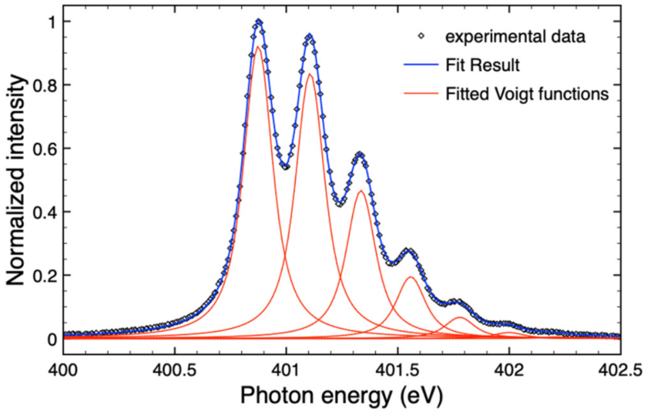

FIG. 5. Nitrogen K-edge absorption spectrum measured with a N_2 gas cell at ALS 6.3.2 beamline. The experimental data (open dots) were fitted using a sum (blue line) of seven Voigt functions (red lines) with the FWHM values of 130 and of 77.8 meV for the Lorentzian and the Gaussian distributions, respectively.

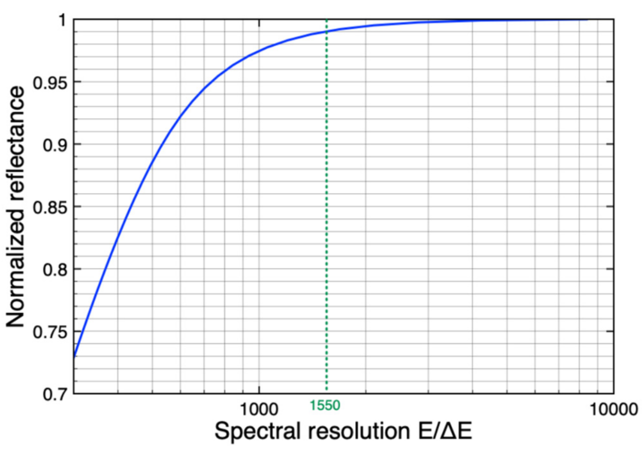

FIG. 4. Effect of instrumental spectral resolution on the peak reflectance R_{peak} calculated from simulations of the multilayer response. For spectral resolution $DE/E \geq 1550$ (dotted line), R_{peak} would be measured with less than 1% error.

The spectral resolution at BESSY II Optics BL estimated by raytracing based on experimental results from commissioning was found to be about 5350 and 2650 with exit slits of 50 μm and 100, respectively. A value of about 5000 has been confirmed using N_2 gas cell measurements with a procedure similar to the one described in Fig. 5.[28] We also checked experimentally that the R_{peak} value does not change significantly when measured with either 50 or 100 μm exit slit [Fig. 6(a)]. This confirms the effect of instrumental spectral resolution on the reflectance spectra measured at the BESSY II beamline is negligible.

The theoretical resolving power during the experiments at SOLEIL is much lower than that at ALS or BESSY because of the low line density grating and large exit slit used. It is estimated to be about 760. This value is well below the 1550 limit plotted in Fig. 3 and may explain why the measured R_{peak} is only 32% for this measurement. Indeed, as shown in Fig. 6(b), if we convolve BESSY data with a Gaussian of 0.52 eV FWHM (corresponding to a resolving power of ∼760), we obtain a good agreement with SOLEIL reflectance spectra. Furthermore, we have observed an increase in R_{peak} while using a narrower exit slit: we were able to measure a reflectance of 33% with a 100 μm exit slit. With an exit slit narrower than 100 μm, however, the signal-to-noise ratio decreases and the

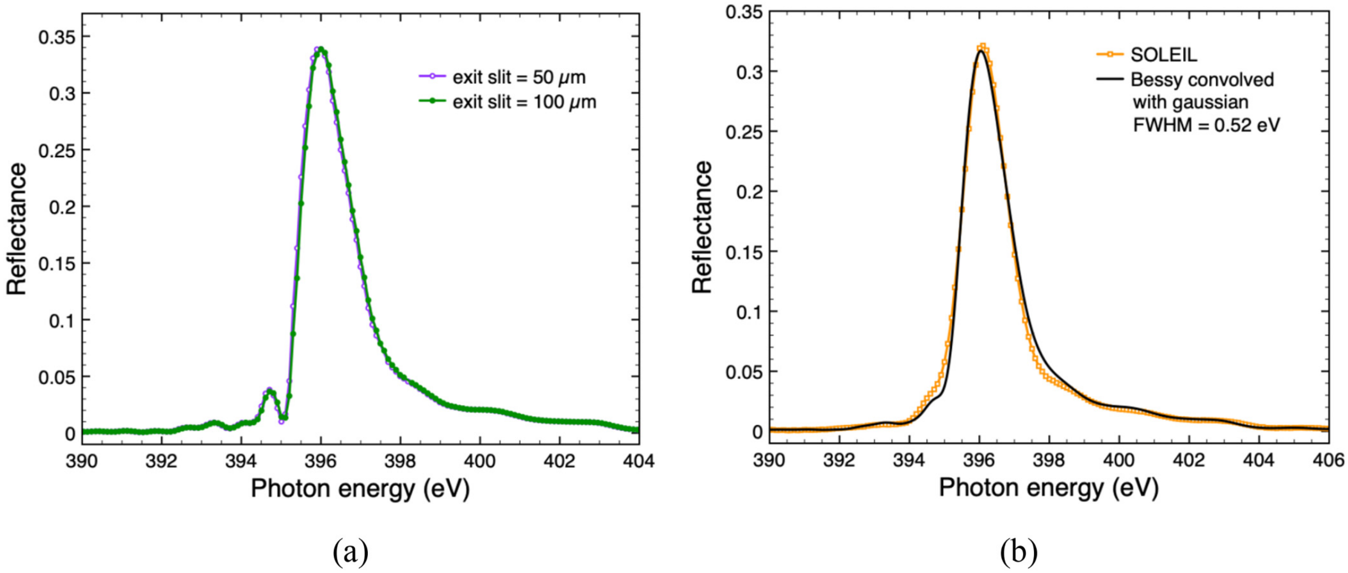

FIG. 6. (a) Reflectance spectra of sample MP23034 measured with 50 (open purple dots) and 100 μm (green dots) exit slit at BESSY; (b) reflectance spectra of sample MP23034 measured at SOLEIL (orange dots) compared to BESSY data convolved with a Gaussian of FWHM = 0.52 eV (black line).

determination of R_{peak} becomes less accurate. Finally, the fact that the Kiessig fringes in SOLEIL spectra are not as well resolved as the ones in ALS and Bessy spectra (see Fig. 2) also confirms the lower spectral resolution, which is responsible for the lower R_{peak} value measured at SOLEIL.

IV. EFFECT OF ANGULAR RESOLUTION (BEAM DIVERGENCE)

Considering vertical divergence (in the plane of incidence for the third beamlines), the angle of incidence on the mirror varies from $\theta - \frac{\text{div}}{2}$ to $\theta + \frac{\text{div}}{2}$, which induces a variation in the Bragg peak energy of DE_{div}. We can connect these two quantities by using Bragg's law, which leads to the following equation:

$$\frac{E}{\Delta E_{div}} \approx \frac{1}{div \times \tan\theta}. \quad (1)$$

For an incidence angle $q = 2.5°$, we obtain $E/DE_{\text{div}} \approx 22\,900/$ *div* (mrad), which is much higher than the spectral resolution for the values of divergence used in this study. Indeed, the vertical divergences reported in Table I for SOLEIL, BESSY, and ALS beamlines induce, respectively, a shift of the peak energy of 9, 12, and 17 meV (i.e., less than 1.2% of the peak bandwidth). Consequently, the effect on the R_{peak} value is negligible (estimated to be <0.01% relative).

We also confirm this theoretical calculation with experimental data shown in Fig. 7, where we compare the reflectance measured at BESSY with two different values of divergence. The slight difference in R_{peak} is below the uncertainty of measurement for this beamline.

The effect of the horizontal divergence a (normal to the incidence plane) is dampened by geometrical consideration: the variation in the angle of incidence on the mirror Dq is given in this case by $\Delta\theta = \tan^{-1}(\tan\theta \times \cos\alpha)$. With the values of horizontal divergence reported in Table I, we obtain a variation in the angle of incidence at least 10 times smaller than in the case of vertical divergence. Consequently, the effect of horizontal divergence on R_{peak} can be neglected as well.

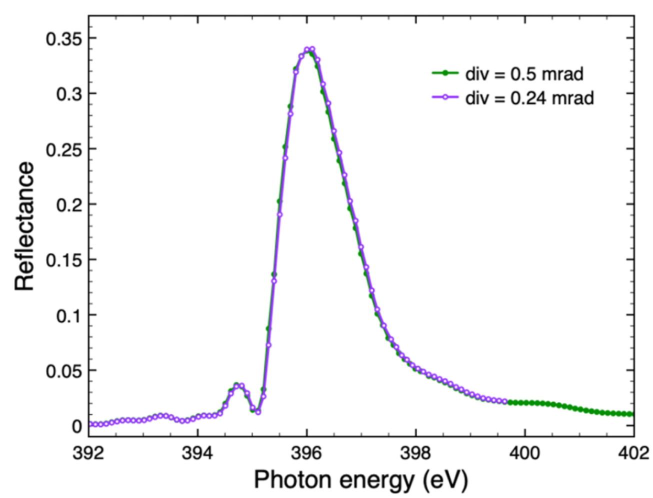

FIG. 7. Effect of vertical divergence on the measured reflectance spectra (BESSY II).

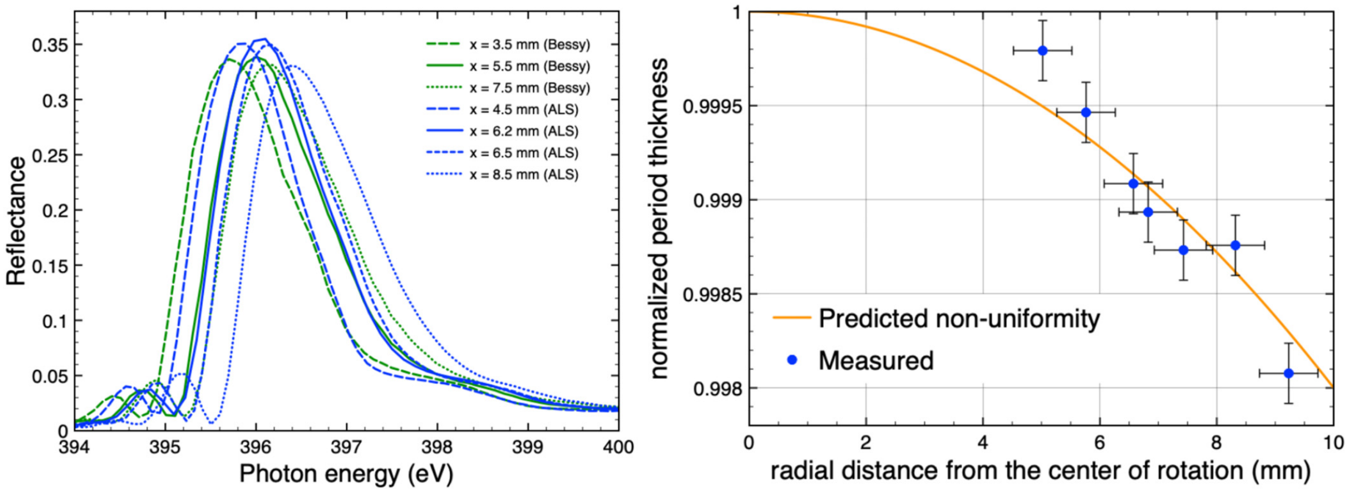

(a) (b)

FIG. 8. (a) Reflectance spectra measured for different spot positions on sample MP23034; (b) normalized period thickness deduced from the energy position of the Bragg peaks as a function of distance to the center of rotation of the sample holder during deposition (blue dots). The orange line corresponds to the predicted non-uniformity for the deposition system.

V. EFFECT OF LATERAL THICKNESS GRADIENT ON THE SAMPLE

The CrN/B_4C/Sc multilayer mirror studied here (sample MP23034) has been deposited by magnetron sputtering. The geometry of the deposition machine has been described in Ref. 29. The spinning of the sample holder assures a good azimuthal uniformity of the deposition. When using standard deposition parameters (i.e., without any uniformity correction), the radial thickness gradient has been measured and is given by in the following equation, where $e(r)$ is the thickness at a radius r from the center of rotation and r is expressed in mm:

$$\frac{e(r)}{e(0)} = 1 - 2.10^{-5}\, r^2. \qquad (2)$$

The radial uniformity calculated from Eq. (2) for a sample of 20 mm is about ±0.1%, which corresponds to ±1.5 pm for sample MP23034.

Usually, for multilayer mirror in the EUV spectral range, we can neglect the effect of this very small non-uniformity on the measured reflectance spectra. Nevertheless, in the WW, because the Bragg peak is very narrow, such a small non-uniformity may impact the result.

In Fig. 8(a), we have plotted the reflectance spectra of sample M23034 measured at different spot locations at ALS and BESSY. The corresponding values of Bragg peak energy are given in Table II. We can see a significant shift in the Bragg peak energy when the spot position is translated up to 5 mm. The normalized period thickness $e(r)/e(0)$ was deduced from the energy position of these Bragg peaks and plotted in Fig. 8(b) as a function of radial distance from the center of rotation (r). The spot locations of Fig. 8(a) correspond to values of r in between 5 and 9.2 mm. The theoretical non-uniformity calculated from Eq. (2) is in good agreement with these experimental results. For each experimental point, we can calculate the gradient slope $de(r)/dr$. As described in Table II, these values range from 0.02 to 0.037%/mm.

With a spot size of ∼100 μm, the energy shift of the Bragg peak within the spot size is less than 15 meV (∼1% of the FWHM of the peak) and the effect on the measured R_{peak} is negligible. Nevertheless, for a larger spot size, we can anticipate a slight decrease in the measured R_{peak}. With the spot size used during BESSY II experiments (350 μm), the shift of the Bragg peak may reach up to 50 meV and we estimated the corresponding reduction in the measured R_{peak} to be about 0.3% (relative).

TABLE II. Effect of the variation in period thickness within the spot for different locations of spot on the sample.

Position × mm	Radius r (mm)	Peak energy (eV)	Gradient coefficient	Gradient slope (%/mm)
3.5	5.02	395.72	0.9995	0.020
4.5	5.76	395.85	0.9993	0.023
5.5	6.57	396.00	0.9991	0.026
6.2	6.83	396.06	0.9991	0.027
6.5	7.43	396.14	0.9989	0.030
7.5	8.32	396.13	0.9986	0.033
8.5	9.23	396.40	0.9983	0.037

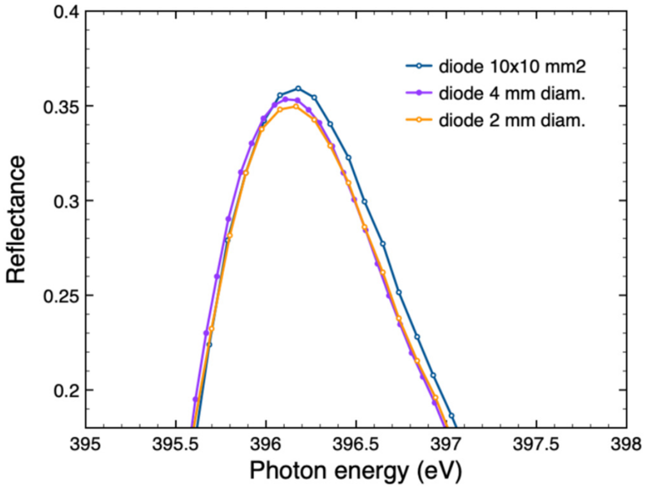

FIG. 9. Comparison of reflectance measurements with three different detector apertures (ALS).

VI. EFFECT OF DIFFUSE SCATTERING FROM THE SAMPLE

At EUV wavelengths, the effect of diffuse scattering from a Mo/Si multilayer on the specular reflectance measurement has been studied and was found to be negligible.[30,31] However, as the wavelength decreases toward the WW, the total integrated scattering increases as $1/l^2$. Thus, the scattered light from the multilayer sample in the WW is expected to be much higher than in the EUV. We conducted an experimental study at ALS 6.3.2 beamline to estimate the impact of this scattered light on specular reflectance measurements by changing the detector aperture. In Fig. 9, we compare the reflectance spectra of sample MP23034 measured with three different detector apertures: $10 \times 10\ \mathrm{mm}^2$ (i.e., the full diode active area), 4 mm in diameter, and 2 mm in diameter. This corresponds to angular aperture in the vertical direction of about 2.36°, 0.97°, and 0.5°, respectively. As shown in Fig. 9, the R_{peak} value decreases from 0.359 to 0.35 when the diode aperture decreases. Thus, the diffuse scattering from the sample in the angle range Dq = 0.5°–2.36° is about 1% of the incident flux.

Figure 10(a) shows an atomic force microscopy image of the multilayer sample surface, and Fig. 10(b) shows the power spectral density calculated from this $1 \times 1\ \mu\mathrm{m}^2$ image. The rms roughness value calculated on the whole spatial frequency range is $s = 0.23$ nm. The relation between the scattering angle q and the spatial frequency f is given by $\sin q = l\, f$. The rms roughness value calculated on the spatial frequency range corresponding to scattering angles in between 0.5° and 2.36° is $s_{eff} = 0.056$ nm. The amount of diffuse scattering from this surface can be estimated with the corresponding Strehl ratio (SR), which represents the ratio of encircled energy between the 2 and the 10 mm diodes:[31] $\mathrm{SR} = \exp[-(4ps_{eff}/l)^2]$. This calculation indicates that ∼1.9% of the incident beam would be scattered in the angles between 0.5° and 2.36°. This value is of the same order of magnitude as the 1% deduced from the measured peak reflectance at ALS (Fig. 9). The discrepancy between the two values can be explained by the fact that the assumption of small roughness ($4ps/l \ll 1$) is not fully satisfied in

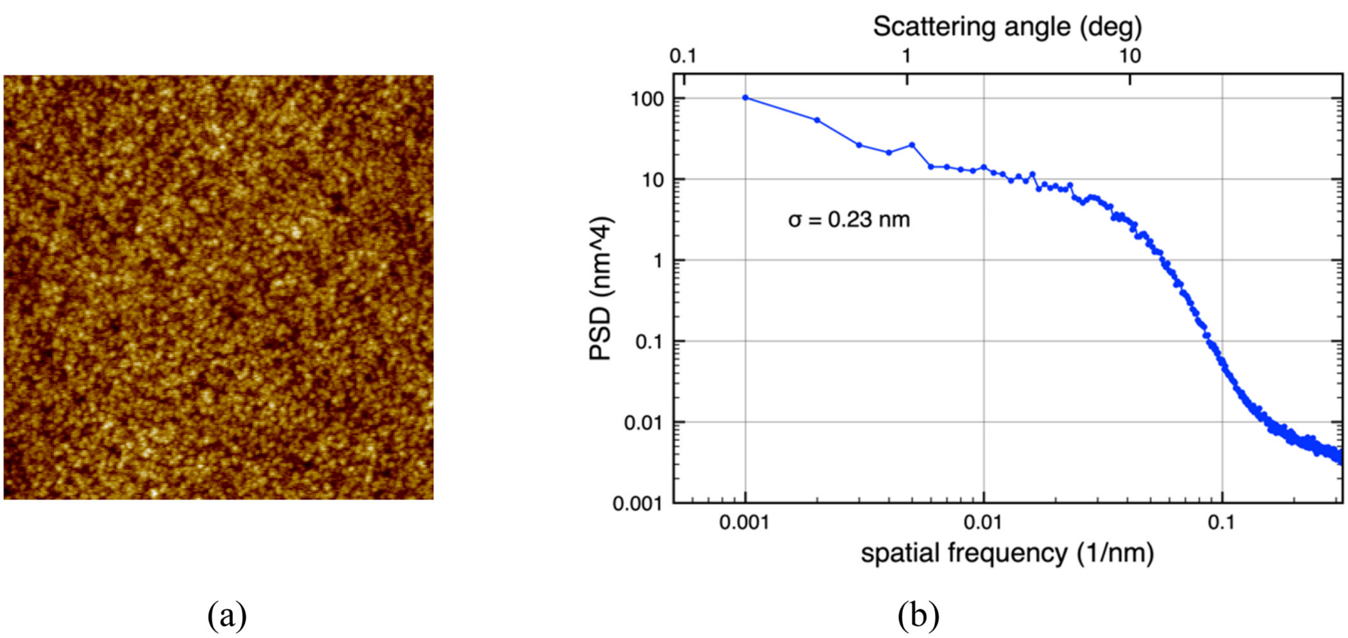

FIG. 10. (a) Atomic force microscopy image ($1 \times 1\ \mu\mathrm{m}^2$) of sample MP23034. (b) Power spectral density of the surface height defects calculated from the AFM image.

this case. The AFM results confirm that the light scattered by the multilayer sample at the angle corresponding to photodiode apertures generally used on synchrotron metrology beamlines is not negligible in the water window spectral range.

VII. CONCLUSION

The reflectance spectra of a $CrN/B_4C/Sc$ multilayer mirror with 500 periods of ∼1.57 nm have been measured at near-normal incidence in the water window at three different synchrotron beamlines: SOLEIL XUV Metrology, ALS 6.3.2 and BESSY II Optics beamlines. The difference in the peak reflectance measured at the three beamlines reveals that specific issues related to the short wavelength range and the large number of multilayer periods have to be addressed for an accurate at-wavelength metrology of high-reflectance multilayers in the water window. Thus, we have studied the potential source of bias in the reflectance measurements by comparing the main characteristics of the three beamlines and by means of theoretical calculations and simulations. We have demonstrated that the spectral resolution of the beamline E/DE needs to be higher than ∼1500 in order to measure the peak reflectance with an error less than 1% (relative). The effect of angular resolution due to beam divergence (in both horizontal and vertical planes) on the peak reflectance was found to be negligible for the three beamlines. The small lateral non-uniformity of the sample due to the deposition process (about 0.2% variation in the multilayer period over 10 mm) was clearly evidence by measuring the reflectance spectra at different locations on the sample. The effect of this non-uniformity on the peak reflectance value (due to the variation in the multilayer period within the spot size) was found to be negligible if the spot size is less than ∼100 μm. We also showed that the light scattered by the multilayer sample can affect significantly the measured peak reflectance value, depending on the photodiode angular aperture. This is because the photodiode collects both the specular and diffuse scattering from the multilayer. These results, confirmed by AFM measurements of the multilayer surface, highlight the necessity to define a criterion on the photodiode aperture for the measurement of R_{peak} in the water window spectral range. Finally, the reflectance of the $CrN/B_4C/Sc$ multilayer mirror was measured at ALS 6.3.2 beamline with a photodiode aperture of 0.5°: we obtained a peak reflectance of 0.35 at l = 3.13 nm (E = 396 eV), which is the highest near-normal incidence reflectance reported for the water window spectral range. The repeatability of the measurements at ALS 6.3.2 beamline was estimated to be ±0.062 pm for the wavelength positioning and ±0.08% for the peak reflectance. This study also confirms the good temporal stability of $CrN/B_4C/Sc$ multilayer coatings over several years.

ACKNOWLEDGMENTS

Funding for this work was provided, in part, by CNRS International Research Project "IRP EREUS."

AUTHOR DECLARATIONS

Conflict of Interest

The authors have no conflicts to disclose.

Author Contributions

Franck Delmotte: Conceptualization (lead); Data curation (lead); Formal analysis (lead); Funding acquisition (lead); Investigation (equal); Methodology (equal); Project administration (lead); Supervision (equal); Validation (lead); Visualization (lead); Writing – original draft (lead); Writing – review & editing (equal). **Evgueni Meltchakov:** Investigation (equal); Resources (equal); Validation (equal); Writing – review & editing (equal). **Andrey Sokolov:** Investigation (equal); Validation (equal); Writing – review & editing (equal). **Pascal Mercère:** Investigation (equal); Writing – review & editing (equal). **Blandine Capitanio:** Investigation (equal). **Eric Gullikson:** Conceptualization (equal); Investigation (equal); Methodology (equal); Supervision (equal); Validation (equal); Writing – review & editing (equal).

DATA AVAILABILITY

The data that support the findings of this study are available from the corresponding author upon reasonable request.

REFERENCES

[1] N. N. Salashchenko and E. A. Shamov, Opt. Commun. **134**, 7 (1997).
[2] F. Schäfers, H.-C. Mertins, F. Schmolla, I. Packe, N. N. Salashchenko, and E. A. Shamov, Appl. Opt. **37**, 719 (1998).
[3] H. Stollberg, S. Yulin, P. A. C. Takman, and H. M. Hertz, Rev. Sci. Instrum. **77**, 123101 (2006).
[4] K. Le Guen, H. Maury, J.-M. André, P. Jonnard, A. Hardouin, F. Delmotte, and M.-F. Ravet-Krill, Appl. Phys. Lett. **91**, 234104 (2007).
[5] A. Hardouin, F. Delmotte, M. F. Ravet, F. Bridou, A. Jerome, F. Varnière, C. Montcalm, S. Hedacq, E. Gullikson, and P. Aubert, J. Vac. Sci. Technol. A **26**, 333 (2008).
[6] A. Guggenmos, R. Rauhut, M. Hofstetter, S. Hertrich, B. Nickel, J. Schmidt, E. M. Gullikson, M. Seibald, W. Schnick, and U. Kleineberg, Opt. Express **21**, 21728 (2013).
[7] M. Prasciolu, A. F. Leontowich, K. R. Beyerlein, and S. Bajt, Appl. Opt. **53**, 2126 (2014).
[8] S. de Rossi, C. Bourassin-Bouchet, E. Meltchakov, A. Giglia, S. Nannarone, and F. Delmotte, Opt. Lett. **40**, 4412 (2015).
[9] M. Kördel, A. Dehlinger, C. Seim, U. Vogt, E. Fogelqvist, J. A. Sellberg, H. Stiel, and H. M. Hertz, Optica **7**, 658 (2020).
[10] C. Nannini, N. Ravinet, E. Meltchakov, C. Gollwitzer, T. N. Tran Caliste, A. Lejars, and F. Delmotte, Opt. Lett. **50**, 6513 (2025).
[11] K. Sakano and M. Yamamoto, Proc. SPIE **3767**, 238 (1999).
[12] F. Eriksson, N. Ghafoor, F. Schäfers, E. M. Gullikson, S. Aouadi, S. Rohde, L. Hultman, and J. Birch, Appl. Opt. **47**, 4196 (2008).
[13] S. Yulin, T. Feigl, and N. Kaiser, "High-performance Cr/Sc multilayers for the soft x-ray range," Proc. SPIE **5963**, 59631T (2005).
[14] E. Gullikson, F. Salmassi, A. L. Aquila, and F. Dollar, paper presented at PXRMS Conference, Presentation S8 O_4, Sapporo, Japan, 12–16 March 2006.
[15] N. Ghafoor, F. Eriksson, E. Gullikson, L. Hultman, and J. Birch, Appl. Phys. Lett. **92**, 091913 (2008).
[16] C. Burcklen, S. de Rossi, E. Meltchakov, D. Dennetière, B. Capitanio, F. Polack, and F. Delmotte, Opt. Lett. **42**, 1927 (2017).
[17] E. Meltchakov, B. Capitanio, S. de Rossi, I. Papagiannouli, P. Mercère, and F. Delmotte, Opt. Lett. **49**, 3420 (2024).
[18] M. Idir, P. Mercere, T. Moreno, and A. Delmotte, Synchrotron Radiat. News **19**, 18 (2006).
[19] J. H. Underwood and E. M. Gullikson, J. Electron Spectrosc. Relat. Phenom. **92**, 265 (1998).

[20]E. M. Gullikson, S. Mrowka, and B. B. Kaufmann, Proc. SPIE **4343**, 363 (2001).
[21]A. Sokolov, M. G. Sertsu, A. Gaupp, M. Lattecke, and F. Schaefers, J. Synchrotron Radiat. **25**, 100 (2018).
[22]A. A. Sokolov, F. Eggenstein, A. Erko, R. Follath, S. Künstner, M. Mast, J. S. Schmidt, F. Senf, F. Siewert, T. Zeschke, and F. Schäfers, Proc. SPIE **9206**, 92060J (2014).
[23]F. Delmotte, J. Meyer-Ilse, F. Salmassi, R. Soufli, C. Burcklen, J. Rebellato, A. Jérome, I. Vickridge, E. Briand, and E. Gullikson, J. Appl. Phys. **124**, 035107 (2018).
[24]D. L. Windt, Comput. Phys. **12**, 360 (1998).
[25]B. L. Henke, E. M. Gullikson, and J. C. Davis, At. Data Nucl. Data Tables **54**, 181 (1993).
[26]M. Kato, Y. Morishita, M. Oura, H. Yamaoka, Y. Tamenori, K. Okada, T. Matsudo, T. Gejo, I. H. Suzuki, and N. Saito, J. Electron Spectrosc. Relat. Phenom. **160**, 39 (2007).
[27]M. Vondrácek, K. C. Prince, J. Karvonen, M. Coreno, R. Camilloni, L. Avaldi, and M. D. Simone, Synchrotron Radiat. News **12**, 27 (1999).
[28]F. Schäfers, P. Bischoff, F. Eggenstein, A. Erko, A. Gaupp, S. Künstner, M. Mast, J.-S. Schmidt, F. Senf, F. Siewert, A. Sokolov, and T. Zeschke, J. Synchrotron Radiat. **23**, 67 (2016).
[29]J. Gautier, F. Delmotte, M. Roulliay, F. Bridou, M.-F. Ravet, and A. Jérome, Appl. Opt. **44**, 384 (2005).
[30]E. M. Gullikson, D. G. Stearns, D. P. Gaines, and J. H. Underwood, Proc. SPIE **3113**, 412 (1997).
[31]E. M. Gullikson, SPIE **3331**, 72 (1998).